

# Supplementary Materials for: Towards a global database of rainfall-induced landslide inventories: first insights from past and new events

Odin Marc<sup>1</sup>, André Stumpf<sup>1</sup>, Jean-Philippe Malet<sup>1</sup>, Marielle Gosset<sup>2</sup>, Taro Uchida<sup>3</sup>, and Shou-Hao Chiang<sup>4</sup>

<sup>1</sup>École et Observatoire des Sciences de la Terre – Institut de Physique du Globe de Strasbourg, Centre National de la Recherche Scientifique UMR 7516, University of Strasbourg, 67084 Strasbourg Cedex, France

<sup>2</sup>Géoscience Environnement Toulouse, Toulouse, France

<sup>3</sup>National Institute for Land and Infrastructure Management, Research Center for Disaster Risk Management, Tsukuba, Japan

<sup>4</sup>Center for Space and Remote Sensing Research, National Central University, Taoyuan City 32001, Taiwan

**Correspondence:** Odin Marc (odin.marc@unistra.fr)

This file contains a supplementary Table listing the imagery used to map landslides and supplementary figure describing:

**Fig S1** the size distribution of landslide for the three different mapping techniques for the Brazil 2011 event.

**Fig S2** the landslide density map for the eight inventories.

5 **Fig S3** the rainfall estimated from satellite during the 2015 Colombia landslide events.

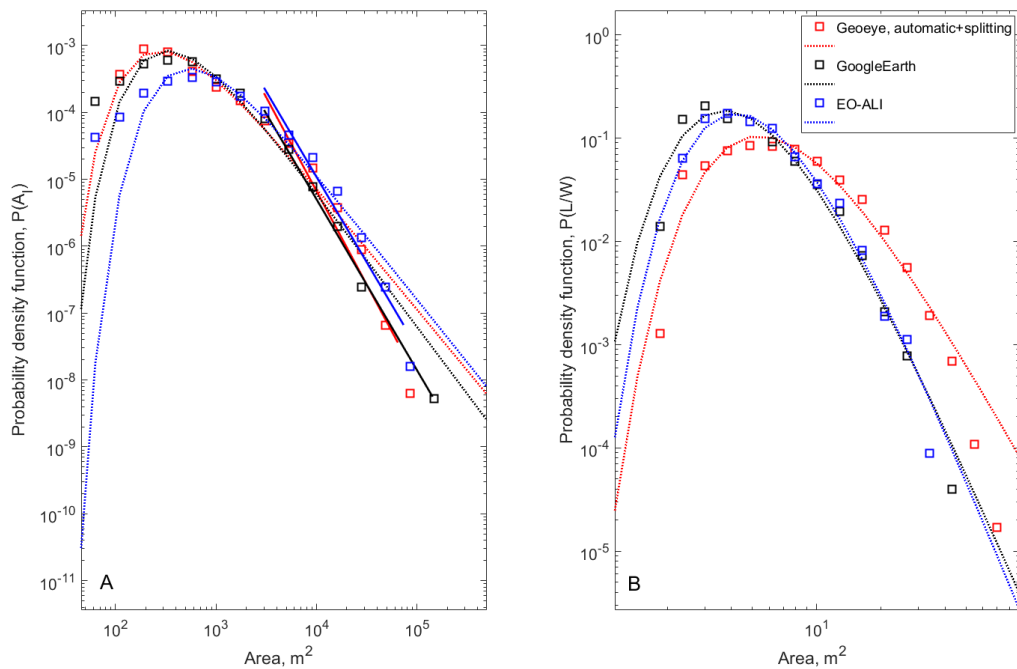
**Fig S4** the length/width ratio distribution and their relation to landslide area for the eight inventories.

**Fig S5** the relation between maximum landslide size and total rainfall.

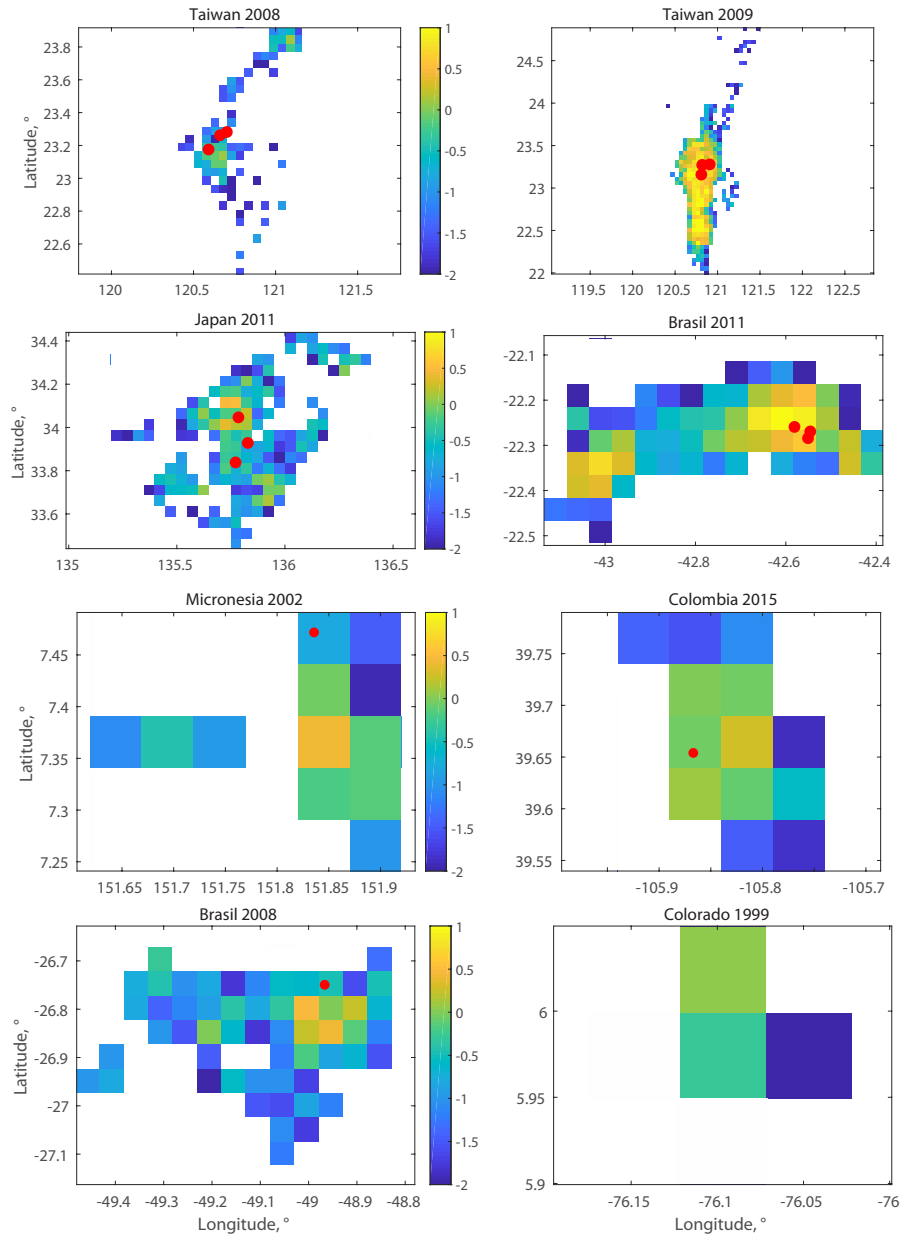
**Fig S6** the landslide distribution of the landslide caused by Typhoon Talas in Japan 2011, and its relation to lithological units.

**Table 1.** Summary of the publicly available imagery accessed to map the rainfall-induced landslides. The format is as follow: Year[Type-Date]. Year is the same as the event when not specified. Image type are abbreviated as L5/8, EO, S2 and GE for Landsat 5/8, EO-ALI, Sentinel-2 and Google Earth. \*\* For Taiwan 2009, Brazil 2011 and Japan 2011, we also accessed Formosat-2, Geoeye-1 and aerial photographs, as described in the main text.

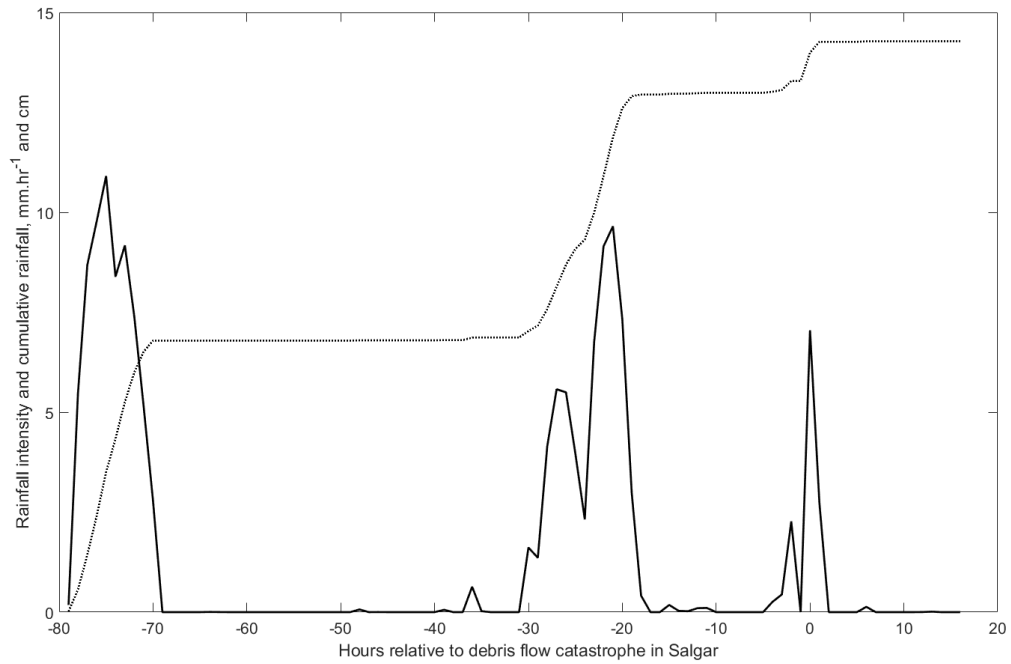
Event	Brazil 2008	Taiwan 2008	Taiwan 2009**	Brazil 2011**	Japan 2011**	Colombia 2015
Pre-event	L5-062	L5-173/196	L5-255	2010[EO-083]; GE	2010[L5-122/154]; L5-196;	2014:[L8-200/361]
Post-event	2009[L5-032]; GE	L5-205	L5-303	EO-033; GE	L5-285/308; GE; 2015[S2-272]	2016[L8-142; S2-203]



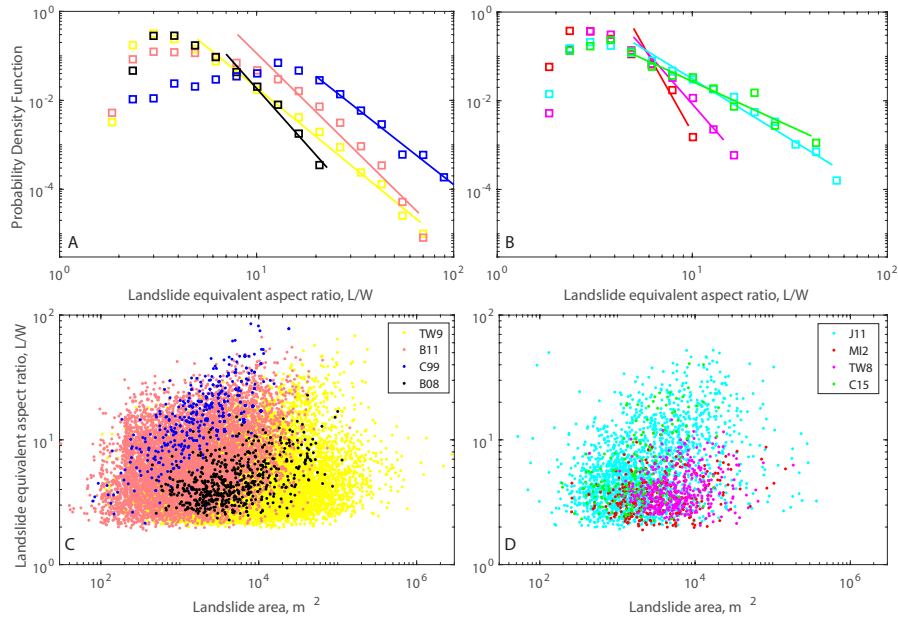
**Supplementary Figure 1.** Probability density functions of landslide area (A) and length/width equivalent ratio (B) for three subareas of the Brazil 2011 event, mapped with different methods: Manually from Google Earth, manually from EO-ALI and with an automatic supervised classification of a very high resolution Geoeeye image, followed by manual splitting and corrections. Dashed lines are maximum likelihood estimation of an Inverse Gamma Distribution associated with each catalog, while solid lines are least square fit of the power-law tails.



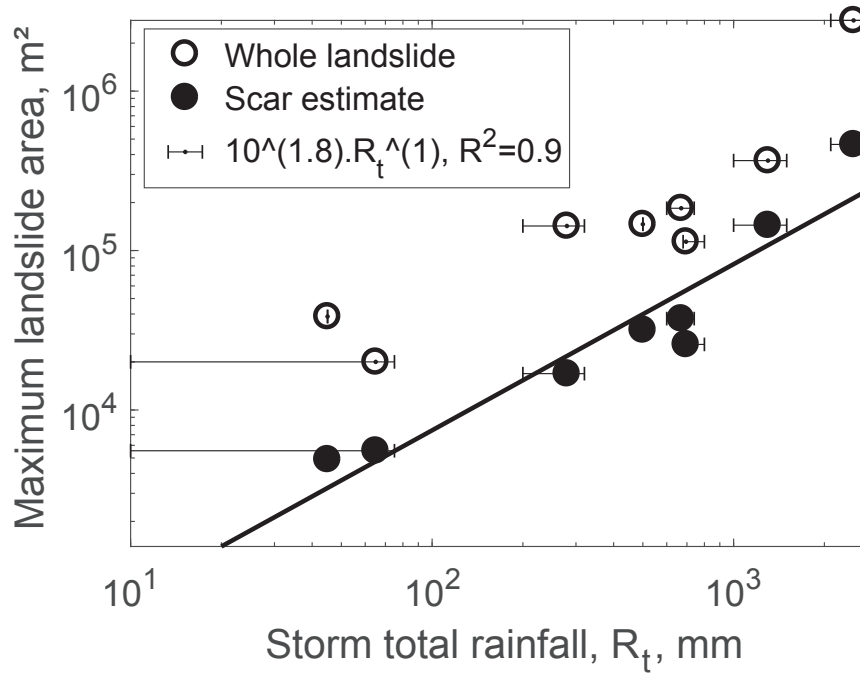
**Supplementary Figure 2.** Map of landslide density (in %) in the affected area of the eight events. Density is computed as the total area of landsliding in a  $0.05 \times 0.05^\circ$  cell divided by the area of the cell. The colorbar indicate the  $\log_{10}$  transformed density. Red dots represent rain gages accessed in this study.



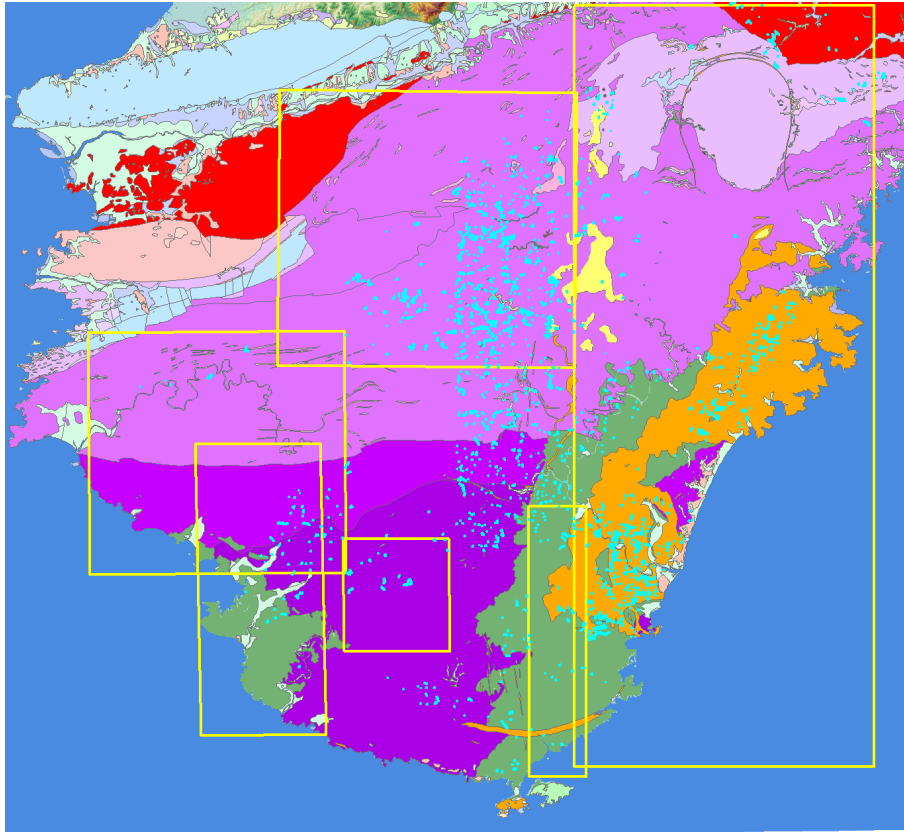
**Supplementary Figure 3.** Rainfall intensity (solid) and cumulative rainfall (dashed) estimates from GSMaP version 7 unaged products. These estimates are based on the average of the four 0.1x0.1° pixel covering the area containing the landslides from the Colombia 2015 event near Salgar.



**Supplementary Figure 4.** Probability density functions of length/width equivalent ratio (A,B) and scatter plot of length/width equivalent ratio against landslide area (C,D) for the 8 landslide inventories. All inventories have a modal L/W of 2-4, except C99 where multiple debris flow were merged and that has a mode beyond 10. Then inventories can be divided in two groups, one where long runout ( $> 10$ ) landslides are rare (Mi2,B08,TW8,C15) while for the others events long runout are much more frequent, including for small landslides.



**Supplementary Figure 5.** Maximum landslide area from the whole landslide or the estimated scar against the total rainfall from the eight inventories.



**Supplementary Figure 6.** Landslide triggered by Typhoon Talas superposed on a simplified geological map. Main lithological units are an Accretionary Melange (4 shades of purple) from Jurassic age (North, light purple), to Miocene age (South, dark purple), Schist (red), Marine Sedimentary rocks (green), volcanic rock (orange) and plutonic intrusion (yellow). Others units North and West are irrelevant to landsliding. Although the relative abundance of landslide in the volcanic zone compared to the neighboring sedimentary zone may relate to rock properties (strength, weatherability), lithology clearly cannot explain the specific landslide pattern within the melange zone.